

# Modeling and Process Operability Analysis of a Direct Air Capture System

Vitor V. Gama\*, San Dinh\*, Victor Alves\*, Beatriz N. A. Dantas\*\*,

Brent A. Bishop\*, Fernando V. Lima\*

*\*West Virginia University, Morgantown, WV 26506, USA*

*(e-mail: fernando.lima@mail.wvu.edu)*

*\*\*Federal University of Campina Grande, Campina Grande, Brazil*

---

**Abstract:** The climate crisis has become an important subject of study since it has impacted every single life on the planet. Aggravated by the large amounts of carbon dioxide released to the atmosphere, such crisis has influenced environmental regulations around the world. To lower the accumulation of this greenhouse gas in the atmosphere, several new technologies are currently being explored in the field of carbon capture and sequestration. This research focuses primarily on Direct Air Capture (DAC) technologies since they have advantages such as ease in installing and placing their facilities. Thus, the capture could be carried out near energy sources and storage sites, hence reducing costs and emissions especially of geographically remote CO<sub>2</sub> producing processes. The DAC system design can be customized to meet the desired CO<sub>2</sub> specifications in the captured product. In this work, a 3-stage membrane module arrangement for DAC is chosen due to its CO<sub>2</sub> separation capabilities. A novel framework based on operability analysis is also employed to find a feasible design region for the DAC system that can operate at different pollution levels. The system is simulated employing AVEVA Process Simulation (an equation-oriented software) coupled with a Python script interface as well as MATLAB to perform process operability calculations. The results show that a feasible design for DAC can be successfully established with the proposed framework accounting for product and byproduct impurities.

---

*Keywords:* Carbon Capture, Membrane Module, Process Operability, AVEVA Process Simulation

---

## 1. INTRODUCTION

The rapid increase in the average temperature of the planet over the past decades has been concerning scientists and policy makers around the world. In particular, Gampe et al. (2021) have discussed future scenarios caused by climate change, such as the increase of heat waves, hotter droughts, and other extreme weather events. Still according to the authors, the planet can store part of the anthropogenic CO<sub>2</sub> produced, gathering 25-30% of the annual emissions. The increasing amount of emissions of this gas has deeply affected the naturally occurring greenhouse effect, and in order to reach the 1.5°C increase scenario set by the Intergovernmental Panel on Climate Change (IPCC), crucial actions must be taken. As stated by Lackner et al. (2012), stabilizing atmospheric carbon dioxide levels requires that emissions from fossil fuels stop or be drastically reduced. In order to meet this goal, Minx et al. (2018) highlighted the importance of conducting research on negative emission technologies (NETs) for direct CO<sub>2</sub> capture from the atmosphere.

The committee on Developing a Research Agenda for Carbon Dioxide Removal and Reliable Sequestration published its agenda (NASEM, 2019) highlighting six major technologies for CO<sub>2</sub> removal: Coastal Blue Carbon, Terrestrial Carbon Removal and Sequestration, Bioenergy with Carbon Capture and Sequestration (BECCS), Direct Air Capture (DAC), Carbon Mineralization and Geologic Sequestration. According to the aforementioned agenda, DAC has the advantage of

being easily installed, reducing work and expenses associated with pipelines connecting the reservoir and the place of capture, and can also produce a product stream at a desirable concentration.

Moreover, Fujikawa et al. (2020) mentioned that DAC technologies have removal capabilities comparable to BECCS (approximately 3.3 Gt-C/year) without the need for large amounts of land and water. Although there is still a lot of research to be done on these technologies, especially regarding the use of membranes, currently they are being treated as a viable option with the U.S. Department of Energy announcing 12 million dollars of funding for DAC (DOE, 2021). Therefore, there is a need for further investigating the potential of DAC in the Process Systems Engineering field.

Motivated by these recent facts, this work aims to find the operable design region for a multistage membrane separation DAC system given a range of pollution level. For simulating this system, an equation-oriented software, AVEVA Process Simulation (APS), is employed as it contains a model library for membrane separation previously developed by the authors (Bishop and Lima, 2020). The developed first-principles model is then used for the operability analysis to find a design region that satisfies all of the output specifications when the CO<sub>2</sub> concentration in the feed air is subjected to a range of disturbances.

## 2. MEMBRANE TECHNOLOGY BACKGROUND

Membrane technologies have been widely studied for gas separation applications. Most membrane systems can be operated continuously, without major use of heating and chemical reactions involved, and also with no addition of chemicals (Favre et al., 2017). In this case, the separation process is characterized purely by mass transfer, resulting in two fractions typically called permeate and retentate, as shown in Figure 1. However, there is a limitation to this type of system, depending on energy requirements when separating a mixture of gases. For example, dilute streams are more difficult to separate and require more energy than more concentrated mixtures (NASEM, 2019).

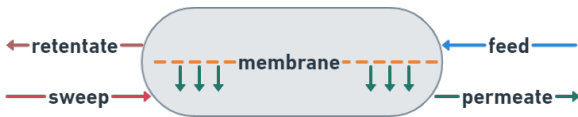


Figure 1. Schematic of the mass transport across a membrane

The use of polymeric membranes is not new to the chemical industry. The first large-scale system for gas separations based on membrane was built in the 80's for hydrogen separation and since then the use of membranes only grew (Clarizia and Bernardo, 2013). In recent years, membrane technologies have shown great potential for CO<sub>2</sub> capture. When compared to other methods, CO<sub>2</sub> capture by permselective membranes may have a low complexity set up and its carbon footprint is small (Fujikawa et al., 2020). Among the commercially available applications for membranes, the hollow-fiber configuration is one of the most industrially applied, according to Gabelman and Hwang (1999). The most relevant characteristics of this type of membranes are covered in the next section.

### 2.1 Hollow fiber membranes

Hollow fiber membranes are designed differently from similar membrane technologies due to their hollow structure instead of the usual flat-sheet structure. Their form allows the construction of compact modules with high membrane surface area; however, the flux across the tubes for these membranes is lower when compared to the flat-sheet membranes (Baker, 2012).

According to Chung et al. (2004), the majority of companies that employ membranes in their processes use hollow fiber membranes due to their module attractive characteristics such as: high surface to volume ratio (e.g., 2000-4000 ft<sup>2</sup>/ft<sup>3</sup>), high membrane packing density and self-support.

### 2.2 Modeling of membrane processes

Favre et al. (2017) emphasized that to accurately evaluate the performance of membranes in gas separation, their behavior must be thoroughly modeled. This model can be started from the cornerstone of membrane technologies, which is the ability to control the amount of permeation of different species in a solution. This ability is expressed by the molar flux shown in equation 1:

$$j_i = \mathbb{P}_i(p_{i_o} - p_{i_i})/l \quad (1)$$

Equation 1 expresses the molar flow of component  $i$  through the membrane in [cm<sup>3</sup> (STP) of component  $i$  / cm<sup>2</sup>.s]. The transport of the component is modeled following Fick's law of diffusion, where  $\mathbb{P}_i$  is the permeability of the component in the membrane material,  $l$  the membrane thickness and the term in the parenthesis is the pressure gradient, in which  $p_{i_o}$  and  $p_{i_i}$  are the partial pressures of the component in either side of the membrane (Baker, 2012). Other important parameters in membrane modeling for gas separation are the selectivity, pressure ratio and stage-cut, shown in equations 2-4, respectively.

$$\alpha_{ij} = \mathbb{P}_i/\mathbb{P}_j \quad (2)$$

$$\varphi = p_o(\text{feed})/p_i(\text{permeate}) \quad (3)$$

$$\theta = \text{permeate flow}/\text{feed flow} \quad (4)$$

In which the selectivity,  $\alpha_{ij}$ , is the capacity of the membrane to separate two different gases, the pressure ratio is the measurement of the extent of the membrane's capacity to perform separation, and lastly, the stage-cut is defined as a ratio between the enrichment of the permeate stream and the removal of the desired component from the feed stream (Baker, 2012). Furthermore, as stated by Kozlova et al. (2018), mathematical modeling is a powerful tool to tackle major tasks in the development and optimization of membrane processes. Still according to the authors, there is a variety of process simulation software available that can accommodate such endeavors in a practical manner.

## 3. PROPOSED APPROACH

### 3.1 System description and modeling

The simulated system corresponds to the 3-stage membrane separation module set up depicted in Figure 2. This set up is adapted from Fujikawa et al. (2020) with the following design and operating conditions assumed:

- Hollow fiber membrane configuration with inner diameter of 1 mm and thickness of 10<sup>-4</sup> mm;
- Mol fraction of CO<sub>2</sub> in the air is evaluated in a range from 400 to 800 ppm;
- CO<sub>2</sub> permeance is of 10,000 gas permeation units (GPU);
- CO<sub>2</sub> concentration of the retentate gas should be ~300 ppm in each stage.
- Pressure of the feed is specified to be 110 kPa and on the permeate side is 2 kPa;

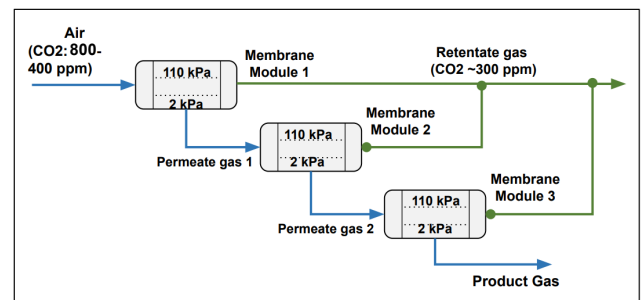


Figure 2. Schematic of direct air capture system modeled based on the work of Fujikawa et al. (2020)

- Membrane flux is proportional to the gradient of the partial pressure of each species.

The 3-stage membrane module arrangement is chosen due to the improved separation of CO<sub>2</sub> when comparing to other configurations (Fujikawa et al., 2020). The information on membrane selectivity and system thermodynamics were also extracted from the aforementioned work. In particular, the selectivity value is set to be 70, and the Peng-Robinson thermodynamic package is used for process simulation. Considering all the specified design and operating conditions, the DAC system is then modeled and simulated in APS, by exploring the existing membrane model library previously developed by the authors (Bishop and Lima, 2020).

### 3.2 Process Operability

Process operability can be a powerful tool to analyze the DAC membrane system in its design phase. In operability analysis, when a first-principles model is available, the relationships between the inputs (physical sizes, manipulated variables, disturbances) and the outputs are represented by the following mapping:

$$y = M(x, u, d) = \begin{cases} \dot{x} = f(x, u, d); x(0) = x_0 \\ y = g(x, u, d) \\ h_1(\dot{x}, x, \dot{u}, u, y, d) = 0 \\ h_2(\dot{x}, x, \dot{u}, u, y, d) \geq 0 \end{cases} \quad (5)$$

in which  $x \in \mathbb{R}^{n_x}$  is the vector of  $n_x$  state variables,  $u \in \mathbb{R}^{n_u}$  is the vector  $n_u$  inputs,  $d \in \mathbb{R}^{n_d}$  is the  $n_d$  vector of process disturbances, and  $y \in \mathbb{R}^{n_y}$  is the  $n_y$  vector of output variables.  $f$  and  $g$  are the nonlinear dynamic mapping equations,  $h_1$  and  $h_2$  are respectively the equality and inequality model constraints.

In this work, the steady-state model of the DAC system is considered for the input-to-output mapping associated with the process operability analysis. Thus,  $u \in \mathbb{R}^{n_u}$  is assumed to be consisted of process design inputs (e.g., membrane areas). The operability sets are defined according to the steady-state model and the following sets:

The Available Input Set (*AIS*) is the set that contains all feasible combinations of the input variables. Mathematically, this set is defined as:

$$AIS = \{u \in \mathbb{R}^{n_u} | u_{min} \leq u \leq u_{max}\} \quad (6)$$

The Expected Disturbance Set (*EDS*) is the set corresponding to all realizations of the disturbances. For the steady-state analysis, the *EDS* is considered to be defined by the boundaries of the disturbance values:

$$EDS = \{d \in \mathbb{R}^{n_d} | d_{min} \leq d \leq d_{max}\} \quad (7)$$

The Achievable Output Set (*AOS*( $d$ )) is the set of reachable output variables that are obtained by substituting all values of the *AIS* into (5). As the outputs are dependent on both the

inputs and the disturbances, the achievable output set at a fixed value of the disturbance is:

$$AOS(d) = \{y \in \mathbb{R}^{n_y} | y = M(u, d); u \in AIS\} \quad (8)$$

The Desired Output Set (*DOS*) is the set of targeted output variables, which represents the required specification of the products. Mathematically, the *DOS* is defined by a set of upper and lower limits as:

$$DOS = \{y \in \mathbb{R}^{n_y} | y_{min} \leq y \leq y_{max}\} \quad (9)$$

The Operability Index (*OI*) is the measurement of the achievable portion of the *DOS*. When the process disturbance is fixed, let  $\mu(S)$  be the hypervolume measure of the set  $S$ , the *OI* is defined as:

$$OI = \mu(AOS \cap DOS) / \mu(DOS) \quad (10)$$

The Desired Input Set (*DIS*( $d$ )) is a subset of the *AIS* that contains all the inputs associated with the outputs in the *DOS*. Since each disturbance value results in a different *AOS*( $d$ ), the Desired Input Set at a fixed value of the disturbance is:

$$DIS(d) = \{u \in \mathbb{R}^{n_u} | y = M(u, d) \in DOS\} \quad (11)$$

In the performed operability analysis of the DAC system, as the inputs are design specifications that are not changeable online, a design of a direct air capture system is valid if and only if its corresponding output vector is contained within the *DOS*. In this case, the Desired Input Set (*DIS*) that satisfies the *DOS* for all values of the disturbances corresponds to the intersection of all the desired input sets *DIS*( $d$ ):

$$DIS = \bigcap_{d \in EDS} DIS(d) \quad (12)$$

## 4. DAC OPERABILITY ANALYSIS RESULTS

After modeling the DAC system in AVEVA Process Simulation, a connection between the process simulator and Python programming language is established to generate the input-output operability mapping. For defining the Available Input Set (*AIS*), the three membrane areas are varied initially by  $\pm 50\%$  of their base-case design values as shown in Table 1. Using this *AIS*, the Achievable Output Set (*AOS*) is calculated as initially a 2D region defined by the CO<sub>2</sub> molar percentage of the CO<sub>2</sub> captured stream and the CO<sub>2</sub> impurity (in parts per million) of the air released. Also, the base-case disturbance scenario of 400 ppm of CO<sub>2</sub> in the process feed stream is assumed for the generation of the input-output data, resulting in a 3x2 (inputs + disturbance x outputs) system.

Using this system, a surrogate model for the DAC process based on Gaussian Process Regression is generated in MATLAB and validated with APS data for further analysis.

The surrogate model is generated for fast computations but also for easy connection to the already developed open-source Operability App in MATLAB (Gazzaneo et al., 2020). This app allows the quantification of achievability of process design regions via Operability Index (OI) calculations.

Table 1: Initial AIS bounds for operability calculations with values within  $\pm 50\%$  of base-case design from the literature

Variable/Bound	Area of 1 <sup>st</sup> membrane [m <sup>2</sup> ]	Area of 2 <sup>nd</sup> membrane [m <sup>2</sup> ]	Area of 3 <sup>rd</sup> membrane [m <sup>2</sup> ]
Lower bound	2.281	0.194	0.027
Upper bound	6.843	0.582	0.081

To quantify the OI, the DOS established is based on CO<sub>2</sub> molar percentages and CO<sub>2</sub> impurities obtained by the base-case design in APS.

The Operability App is then used to generate the AOS from the simulation results for efficient OI calculations. The OI for the base-case disturbance scenario is illustrated in Figure 3, where one can inspect the narrow region of operation for this design (in red), quantified via the OI of 5.595%. This result elucidates the potential challenging operation of the DAC process under the established conditions, in which a considerable portion of the desired operation cannot be reached with the current design and the initial bounds set for the membrane module areas.

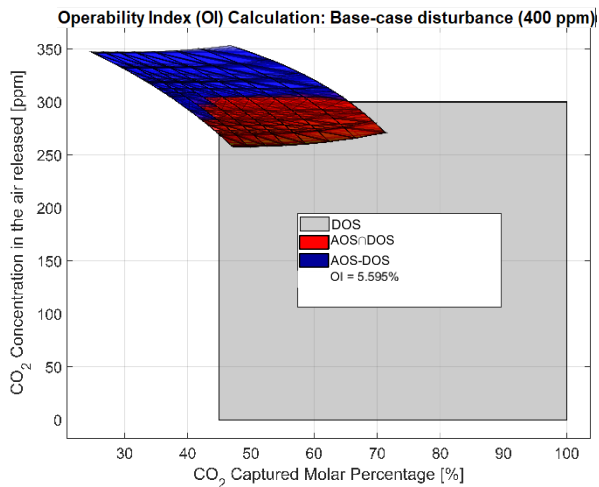


Figure 3: OI calculation for base-case disturbance scenario: 400 ppm of CO<sub>2</sub> in process feed stream

The Operability studies are continued by adjusting the AIS initial bounds in order to find a feasible design region that contains all systems that are able to purify the air considering different CO<sub>2</sub> inlet concentrations, while still maintaining the requirement for the captured byproduct. Thus, the disturbance that was fixed in the initial operability analysis (CO<sub>2</sub> at the inlet stream concentration) is now also incorporated into the operability studies in order to investigate its impact on the design problem. The revised bounds of the AIS for this second study, the EDS and the DOS sets, which are maintained the same from the first study, are depicted in Table 2.

Table 2: Revised AIS and remaining operability sets for the direct air capture system

Revised Available Input Set (AIS)		
Variable	Lower bound	Upper bound
Area of the first membrane [m <sup>2</sup> ]	5.9248	17.8283
Area of the second membrane [m <sup>2</sup> ]	0.5603	1.6809
Area of the third membrane [m <sup>2</sup> ]	0.0831	0.2494
Desired Output Set (DOS)		
CO <sub>2</sub> concentration in the released air [ppm]	0	300
CO <sub>2</sub> concentration in the captured stream (%)	45	100
Expected Disturbance Set (EDS)		
CO <sub>2</sub> concentration in the inlet stream [ppm]	400	800

The operability mapping in this case generates the  $AOS(d)$  by discretizing the inputs and the disturbances and using their values in the steady-state model. In this case study, each input is discretized into ten values that are equally spaced between their boundaries, and the disturbance is discretized into five values that are equally spaced between its boundaries. As a result, five different  $AOS(d)$ s are generated as polytopes and shown in Figure 4, in which the color of each polytope represents one disturbance scenario of the associated  $AOS(d)$ . From visual inspection of this figure, one can conclude that the current AIS is now sufficiently large to find the set of designs that are operable for all values of the disturbance. In other words, the considered ranges of the membrane areas are now large enough to find the feasible regions that can operate for different qualities of the ambient air.

From the intersection of each  $AOS(d)$  with the DOS, an inverse mapping is performed next by looking up the values that satisfy the air quality constraints to find which designs are operable for different values of inlet air quality. The results of the inverse mapping are shown in Figure 5, in which the five transparent polytopes are the  $DIS(d)$  and their colors indicate the values of the respective disturbances.

In the case study of direct air capture, each  $DIS(d)$  is a convex set, thus allowing the set representations with linear inequality constraints. Using set of inequality constraints allow intersections to be computed efficiently by finding all the extreme points of the linear inequality equations from all five  $DIS(d)$ s. In the final step of the steady-state operability analysis, the  $DIS$  intersection of all  $DIS(d)$  is computed. For every point in this calculated  $DIS$ , a design of the 3-stage membrane DAC system with the respective membrane areas is guaranteed to be able to meet the output specifications regardless of the CO<sub>2</sub> concentration considered in the inlet air. Lastly, this calculated  $DIS$  takes the form of  $Au \leq b$ , which is suitable for potential future work that involves implementing

an optimization algorithm (such as MILP) for the DAC system.

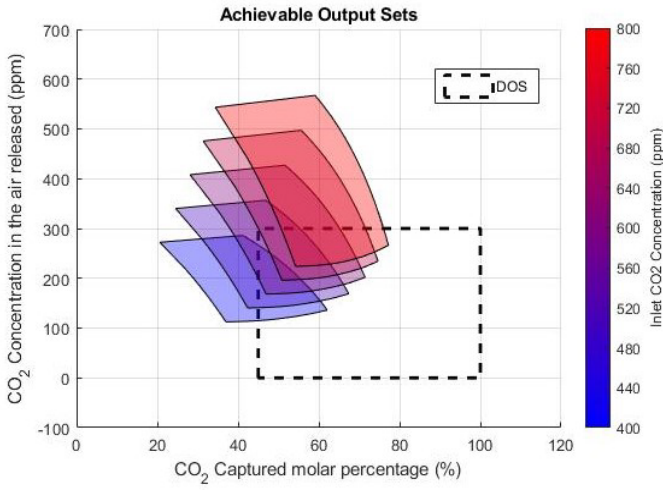


Figure 4: The Achievable Output Sets for five different values of the disturbances

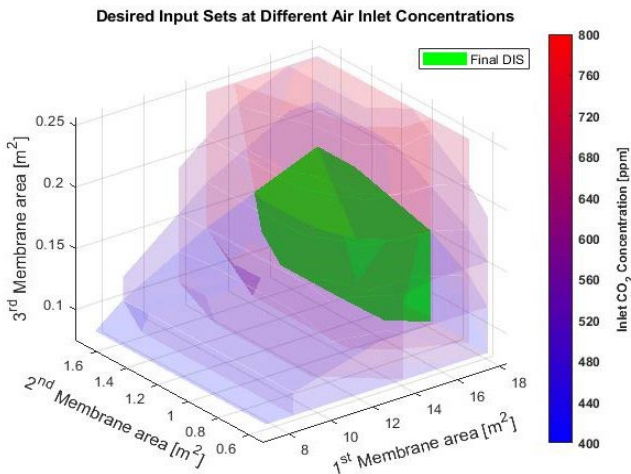


Figure 5: Feasible design space for the DAC system

Further investigation is carried out by including an additional dimension in the output spaces (AOS/DOS), by considering the CO<sub>2</sub> emission per unit energy consumed in the process, following definitions from the U.S Energy Information Administration (EIA) (U.S EIA, 2020). In particular, the AOS/DOS variable analyzed corresponds to the energy efficiency of the DAC system, calculated per unit mass of CO<sub>2</sub> released, as shown in equation (13):

$$Efficiency = \frac{lb. of CO_2}{kWh} [lb/ kWh] \quad (13)$$

The direct operability mapping is then generated for this second 3x3 (inputs + disturbance x outputs) system in order to further investigate if the energy requirements mentioned in the literature are met with this initial AIS region defined. The AIS and AOS considered for this case are shown in Figures 6 and

7, respectively. The color coding of Figures 6 and 7 serves as an indicator for corresponding input and output regions and does not indicate different values. Specifically, the red inputs in Figure 6 map to the red outputs in Figure 7, and other colors designate similar relationships. Note from these figures that the maximum efficiency value that can be achieved for this design corresponds to 0.2 lbCO<sub>2</sub>/kWh, thus not being able to meet the minimum 0.85 lbCO<sub>2</sub>/kWh EIA specification. This indicates that the AIS initial region defined must be expanded to further inspect if the process can meet the target specifications.

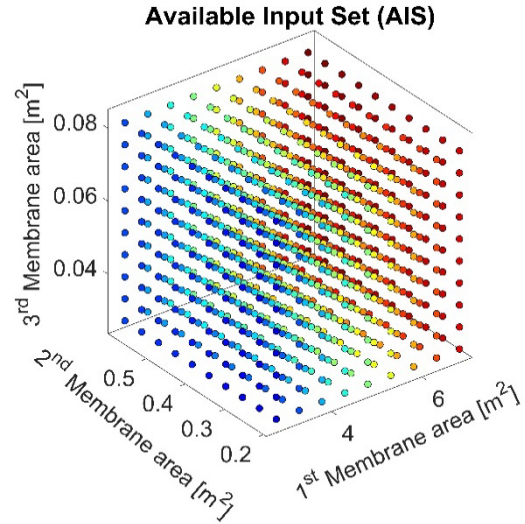


Figure 6: AIS for base-case disturbance scenario: 400 ppm of CO<sub>2</sub> in feed stream

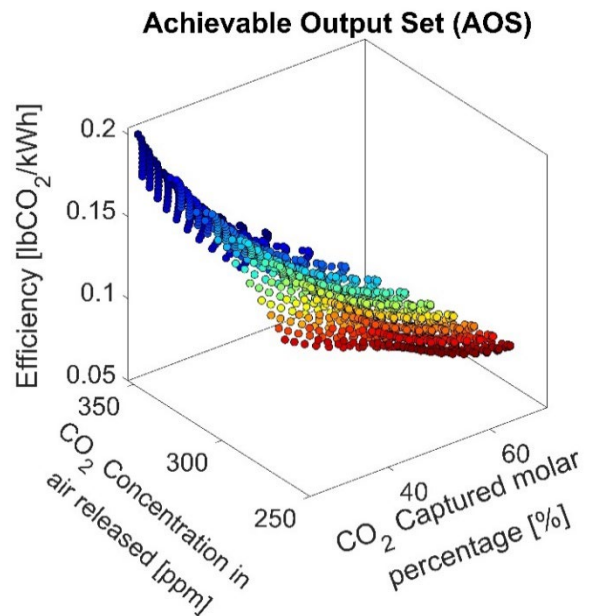


Figure 7: AIS for base-case disturbance scenario: 400 ppm of CO<sub>2</sub> in feed stream

By analyzing the AOS region in Figure 6, it can also be observed that the objective of attaining an efficient DAC process is conflicting with the maximum CO<sub>2</sub> contamination



in the air released at the base-case design (300 ppm), i.e., the higher the efficiency, the more contaminated the air stream becomes. In addition, the system efficiency and the purity of the CO<sub>2</sub> captured are also conflicting goals, as the lower AOS region (in red) with a high CO<sub>2</sub> purity has the lowest efficiency.

The Process Operability analysis can thus show the potential challenges for this initial process design with respect to the energy consumed, indicating the necessity of investigating further arrangements such as heat integration, for example, as an attempt to attain both purity and energy requirements. Lastly, by analyzing Figure 6 with the color-coded mapping that relates Figures 6-7, one can conclude that the region of highest purity of CO<sub>2</sub> (in red) is related to increased membrane areas (also in red), which will impact the equipment costing, and thus the economics of this process.

#### 4. CONCLUSIONS

A process model for the DAC system has been proposed considering a 3-stage module arrangement and operating conditions based on the literature. Process Operability studies were carried out using this model in order to investigate the achievability of the proposed design, considering typical disturbances in the process, CO<sub>2</sub> impurity and captured CO<sub>2</sub> purity streams. Moreover, the energy efficiency of the proposed DAC process was also investigated, seeking insights about feasibility of the current design when compared against EIA targets. The obtained results showed that a feasible design can be established when accounting for products and byproducts impurities. However, further optimization would be needed for improving the design efficiency towards the 0.85 lb CO<sub>2</sub>/kWh goal reported by EIA, which will be subject of future investigation.

#### ACKNOWLEDGMENTS

The authors acknowledge the Statler College of Engineering at West Virginia University and National Science Foundation CAREER Award 1653098 for supporting this research.

#### REFERENCES

- Baker, R. W. (2012). *Membrane Technology and Applications*. Wiley, UK.
- Bishop, B., Lima, F. V. (2020). Modeling, Simulation, and Operability Analysis of a Nonisothermal, Countercurrent, Polymer Membrane Reactor. *Processes*, volume (8), 78.
- Chung, T.-S., Li, D., Wang, R. (2004). Fabrication of lab-scale hollow fiber membrane modules with high packing density, *Separation and Purification Technology*, volume (40), 15-30.
- Clarizia G., Bernardo P. (2013). 30 Years of Membrane Technology for Gas Separation, *Chemical Engineering Transactions*, 32, 1999-2004.
- Favre E., Bounaceur, R., Berger, E., Pfister, M., Santos, A. A. R. (2017). Rigorous variable permeability modelling and process simulation for the design of polymeric membrane gas separation units: MEMSIC simulation tool, *Journal of Membrane Science*, volume (523), 77-9.
- Fujikawa, S., Selyanchyn, R. & Kunitake, T. (2021). A new strategy for membrane-based direct air capture. *Polym. J.*, volume (53), 111–119.
- Gabelman A., Hwang S-T. (1999). Hollow fiber membrane contactors, *Journal of Membrane Science*, volume (159), 61-106.
- Gampe, D., Zscheischler, J., Reichstein, M. et al., (2021). Increasing impact of warm droughts on northern ecosystem productivity over recent decades. *Nat. Clim. Chang.* 11, 772–779.
- Gazzaneo, V., Carrasco, J. C., Vinson, D. R., Lima, F. V. (2020). Process Operability Algorithms: Past, Present, and Future Developments. *Industrial & Engineering Chemistry Research*, volume (59), 2457-2470.
- Han Y., Winston Ho, W.S. (2018). Recent advances in polymeric membranes for CO<sub>2</sub> capture, *Chinese Journal of Chemical Engineering*, volume (26), 2238-2254.
- Kozlova, A.A., Trubyanov, M.M., Atlaskin, A.A. et al., (2019). Modeling Membrane Gas and Vapor Separation in the Aspen Plus Environment. *Membr. Membr. Technol.* volume (1), 1–5.
- Lackner, K. S., Brennan, S., Matter, M. J., Park, A. A.-H., Wright, A., Van der Zwaan, B. (2012). The urgency of air capture. *Proceedings of the National Academy of Sciences*. 109 (33), 13156-13162.
- Minx, J. C., et al., (2018). Negative emissions—Part 1: Research landscape and synthesis. *Environ. Res. Lett.*, volume (13).
- National Academies of Sciences, Engineering, and Medicine. (2019). *Negative Emissions Technologies and Reliable Sequestration: A Research Agenda*. Washington, DC: The National Academies Press.
- U.S Energy Information Administration. FREQUENTLY ASKED QUESTIONS (FAQS) - How much carbon dioxide is produced per kilowatthour of U.S. electricity generation? December 15, 2020. <https://www.eia.gov/tools/faqs/faq.php?id=74&t=11> (accessed on November 5, 2021).
- US Department of Energy. DOE Announces \$12 Million For Direct Air Capture Technology. <https://www.energy.gov/articles/doe-announces-12-million-direct-air-capture-technology> (accessed on October 6, 2021).